

Long Term Evolution of Space Debris Clouds in the Cislunar Region

Sourav Ghosh^{a,*}, Prathap S. Sharma^b, Siddhartha Pundit^c, Rishikesh Bitla^d, Subhasmita Prusty^e, Samarth Badgugar^f

^a*The University of Tokyo, Tokyo, Japan*

^b*ISAE-SUPAERO, Toulouse, France*

^c*Independent Researcher, Bengaluru, India*

^d*Jain (Deemed-to-be University), Bengaluru, India*

^e*VIT Bhopal University, Bhopal, India*

^f*University of Padua, Padua, Italy*

Abstract

As humanity pushes beyond Earth toward a sustained presence around the Moon, we face a familiar problem in a new neighbourhood: space debris. Decades of activity in near-Earth orbits have already filled space with fragments too small to track reliably yet large enough to threaten spacecraft, and if we repeat that pattern in the vast cislunar region between Earth and the Moon, routine lunar operations could become riskier, costlier, and more fragile. This study aims to understand the complex implications of the formation of debris clouds and their evolution in the cislunar space, and how they affect operations near the lunar region. We focus on the orbits most likely to matter, Near-Rectilinear Halo Orbits (planned for NASA's Gateway), a Distant Retrograde Orbit, and a L_2 orbit, and simulate debris created by collisions or explosions, then follow those fragments for months to years. To keep things realistic, the Earth–Moon circular restricted three-body dynamics is used. We quantify the chance that debris ultimately strikes the Moon, and also track how fragments ride natural phase-space “highways,” migrating among orbit families. The result is a set of practical outputs, risk maps, survival timelines, all aimed at informing near-term operations. We close with concrete mitigations operators can adopt now, from keep-out zones and station-keeping choices to safer disposal strategies, so today’s small mishaps don’t become tomorrow’s systemic hazard for the Artemis era.

Keywords: Space Debris, Space Situational Awareness, Cislunar Space

1. Introduction

The cislunar region, the vast expanse between the Earth and Moon, is emerging as the next frontier for space exploration and development. With growing ambitions from governmental space agencies and private enterprises alike, humanity is preparing to establish a sustained presence beyond low Earth orbit. A manned lunar outpost, once a distant aspiration, now lies within reach. To support such a presence, a wide array of space infrastructure will need to be deployed in the cislunar environment. These include communication relays, navigation systems, surveillance platforms, scientific instruments, and logistics modules, all of which will play crucial roles in enabling long-term human operations on and around the Moon. However, as with any

expansion into new orbital regimes, the issue of space debris becomes an inevitable and pressing concern. History has shown us in near-Earth space that operational satellites and platforms are susceptible to malfunctions, fragmentation events, and collisions, all of which generate hazardous debris. In the cislunar region, the problem is compounded by the complex and often chaotic dynamical environment governed by the gravitational interplay between the Earth, Moon, and Sun. These dynamics can cause debris to evolve in unpredictable ways over time, posing significant collision risks not only to other operational assets but also to lunar surface installations and future crewed missions.

This study seeks to address the emerging challenge of debris risk in the cislunar space environment. By modeling and simulating key scenarios, including in-orbit break-up events, high-energy impact trajectories, and long-term orbital evolution, we aim to assess potential debris propagation patterns and their associated hazards. In particular, we investigate how fragments from

*Corresponding author

Email address: sourav.ghosh@space.t.u-tokyo.ac.jp
(Sourav Ghosh)



Figure 1: Illustration of Space Debris by ESA[1]

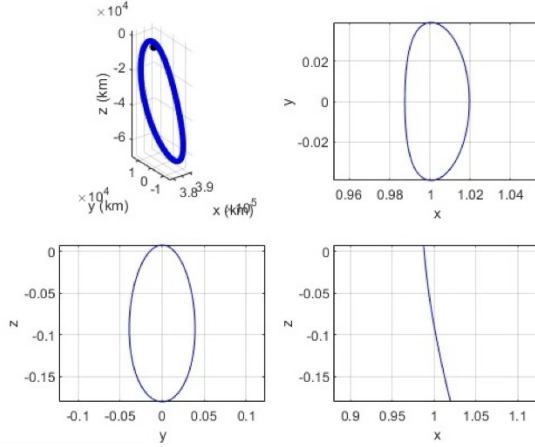


Figure 2: NRHO Orbit

operational failures or collisions might interact with valuable regions such as Earth-Moon Lagrange points, lunar transfer corridors, lunar orbit, and also near-Earth regions such as Geostationary and Geosynchronous orbits. These insights are critical for informing the design of future space traffic management protocols, shielding strategies, and operational policies that will ensure the safety, sustainability, and success of humanity's next great leap into space. Results presented demonstrate the spread of the debris field over time based on Monte-Carlo simulations of a breakup event in the NRHO, a Distant Retrograde orbit (DRO), and a L_2 Halo Orbit.

2. Dynamics Model

2.1. Circular Restricted Three-Body Problem

The complex dynamics of the region can be simplified using the Circular Restricted Three-Body Problem (CR3BP). This model makes the assumptions as follows:

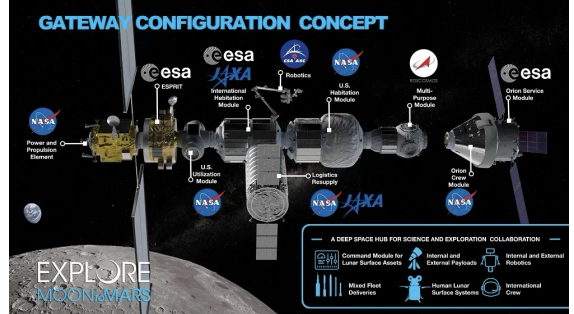


Figure 3: NASA's Lunar Gateway (Artemis Program) [2]

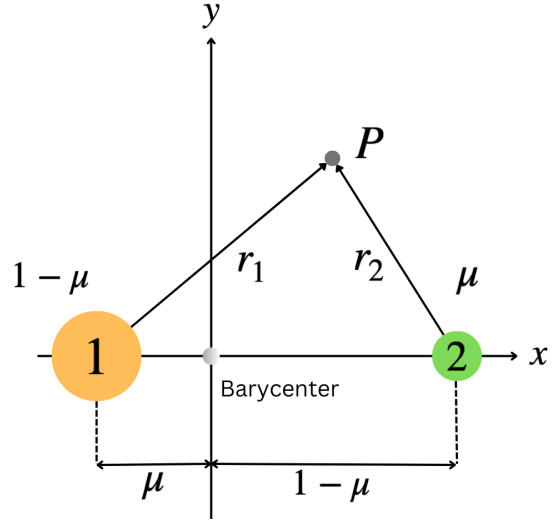


Figure 4: CR3BP Model

- The primary and secondary masses (Earth and Moon) are in a circular orbit around the barycenter of the system.
- The third body is assumed to be a point mass and exerts no force on the other masses.

The system may be described using the following relations [3].

$$\ddot{x} - 2\dot{y} = \Omega_x \quad (1)$$

$$\ddot{y} + 2\dot{x} = \Omega_y \quad (2)$$

$$\ddot{z} = \Omega_z \quad (3)$$

where, Ω is the pseudo-potential given by,

$$\Omega = \frac{1}{2}(x^2 + y^2) + \frac{1-\mu}{r_1} + \frac{\mu}{r_2} \quad (4)$$

$$r_1 = \sqrt{(x + \mu)^2 + y^2 + z^2} \quad (5)$$

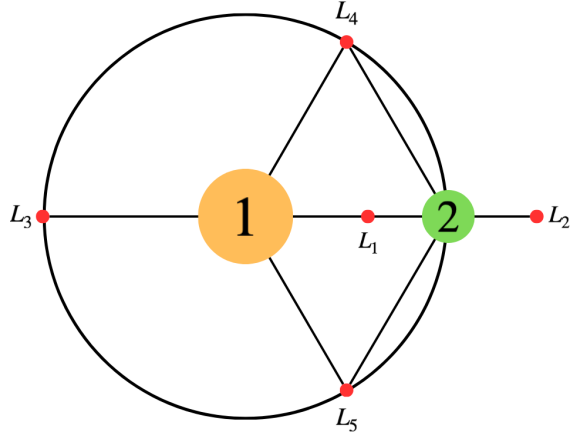


Figure 5: Location of Lagrange Points

$$r_2 = \sqrt{(x - 1 + \mu)^2 + y^2 + z^2} \quad (6)$$

where, μ is the mass parameter defined as,

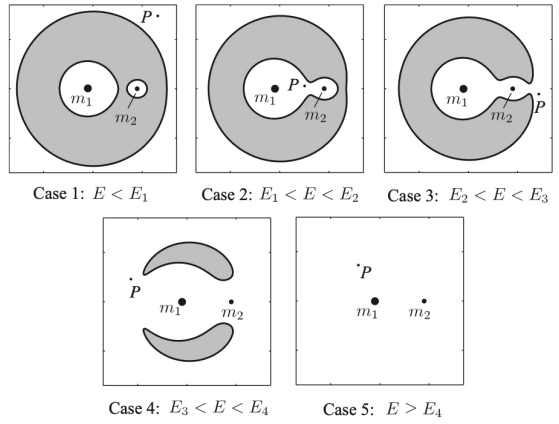
$$\mu = \frac{m_2}{m_1 + m_2} \quad (7)$$

2.2. Realms of Possible Motion

In the Circular Restricted Three-Body Problem (CR3BP), a spacecraft's movement is restricted to specific spatial realms based on its energy level. This energy state is defined by a conserved value called the Jacobi constant, which determines the boundaries of where the craft can physically travel according to the following expression:

$$E = 2\Omega - v^2 \quad (8)$$

Figure 6 illustrates these realms through the use of zero-velocity surfaces (ZVS), which define the physical limits a spacecraft cannot exceed without an injection of energy. Within the rotating reference frame of the Earth–Moon system, the specific shape and reach of these regions are governed by the interplay of gravitational forces and centrifugal potential. Access is strictly governed by the Jacobi constant: motion is only possible in regions where kinetic energy is non-negative, effectively rendering the outside areas "forbidden." In 2D projections, these boundaries appear as zero-velocity curves (ZVCs) that function as dynamic gateways. Depending on the spacecraft's energy level, these gates may open or close, either confining the craft to a local vicinity or permitting transit between different zones, such as moving from Earth's influence to that of the Moon.

Figure 6: Realms of Possible Motion for different Jacobi Constant values E [3]

2.3. Propagator Setup

A Variable-Step, Variable-Order (VSVO) Adams-Basforth-Moulton integrator referred to as ODE113 in MATLAB is used to propagate trajectories.

3. Breakup Simulations

3.1. Fragmentation Modeling

Spacecraft breakup events may be classified into two main types, collisions and explosions. It is very challenging to accurately model a spacecraft breakup event, since it involves several aspects such as the energy released during the event, the materials of the spacecraft, and several other quantities. Based on observations from events in the near-Earth orbits, NASA developed an empirical model referred to as EVOLVE 4.0. This model gives a good estimate of the number of fragments, their size distribution as a function of the parent satellites' size, fragment area and masses, and also the type of event. The characteristic length of any fragment is given by the relation [4]:

$$L_c = \frac{1}{3}(X + Y + Z) \quad (9)$$

Based on this, we may obtain the size distribution of fragments from an explosion and collision event respectively given by [4]:

$$N_{\text{frag}}^{\text{exp}} = 6L_c^{-\beta_{\text{exp}}} \quad (10)$$

$$N_{\text{frag}}^{\text{col}} = 0.1M^{0.75}L_c^{-\beta_{\text{col}}} \quad (11)$$

Initial Debris Positions (CR3BP frame)

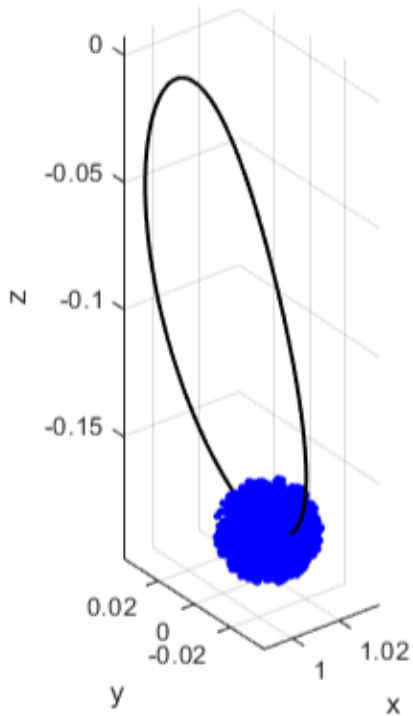


Figure 7: Representation of Initial Debris Positions with NRHO for reference (Debris Field magnified for representation)

where, $\beta_{\text{exp}} = 1.6$ and $\beta_{\text{col}} = 1.71$, and M is the combined masses of the two objects that collided. Subsequently, we may model the area and mass of the fragments using the relations:

$$m_f = \frac{4}{3}\pi\left(\frac{L_c}{2}\right)^3 \rho_f \quad (12)$$

$$A_f = \pi\left(\frac{L_c}{2}\right)^2 \quad (13)$$

Above relations may be further simplified to obtain the Area-to-mass ratio of each fragment, given by the relation:

$$\left(\frac{A}{m}\right)_f = \frac{3}{2} \frac{1}{L_c \rho_f} \quad (14)$$

3.2. Monte-Carlo Simulations of Breakup events

Based on EVOLVE 4.0, Monte-Carlo based simulations are done to generate debris fragments from explosions and collisions, and the spread of fragments post breakup is assumed to be omnidirectional. Hence, a

Δv profile based on the following is imparted on each fragment[4]:

$$\Delta v_x = \Delta v \left(\sqrt{1 - u^2} \right) \cos \theta \quad (15)$$

$$\Delta v_y = \Delta v \left(\sqrt{1 - u^2} \right) \sin \theta \quad (16)$$

$$\Delta v_z = \Delta v u \quad (17)$$

where, u is a random number uniformly sampled between -1 and 1, and θ is a random angle sampled between 0 and 2π . The initial mass of the parent satellite is considered to be 1000 kg, and the characteristic lengths of fragments are sampled between 10 cm and 1 m. 1000 runs were performed, and three main orbits were analyzed, which include the Near-Rectilinear Halo Orbit (NRHO), a Distant Retrograde Orbit (DRO), and a L₂ Halo orbit. Each fragment is then propagated over a period of 3, 6, 9, 12, and 60 months to demonstrate their behaviour over a long duration of time. The initial fragment positions are randomized within a sphere of radius 500 m about the parent state, with this perturbation implemented in the nondimensional CR3BP rotating frame by scaling the physical radius by the characteristic length unit (LU), i.e., $\delta r_{nd} = 500\text{m}/\text{LU}$ (with LU taken as the Earth–Moon distance).

3.3. Collisions with the Moon

Upon propagation, Fragments that impact the Moon are flagged. This helps with assessing the collision risk, and also the potential risks of debris in the region.

4. Simulations

As stated in sections 3.2 and 3.3, 1000 Monte-Carlo runs of debris are propagated for each of the orbits studied, and collisions are flagged. A heatmap of fragment location after each time step is generated, which is used to determine the evolution of the debris cloud over a duration of five years. Results are as seen in the following figures. Figures 8, 9, and 10 are corresponding heatmaps of fragment positions after certain periods of time, propagated as stated in section 2.3. Results from corresponding simulations are as discussed below.

4.1. Near Rectilinear Halo Orbits

A total of 629361 fragments of debris were simulated, and it was determined that at least 130719 fragments of debris struck the surface of the moon over the entire simulation period. Due to the close proximity of the orbit to the moon's surface, this result was expected.

Table 1: Initial Conditions of Orbits studied

Orbit Type	x	y	z	\dot{x}	\dot{y}	\dot{z}	T_{period}	E
NRHO	1.01949	0.0	-0.18029	0.0	-0.09768	0.0	1.47	3.049091
DRO	0.38681	0.0	0.0	0.0	1.60446	0.0	6.15	2.567900
L ₂ Halo Orbit	1.08958	0.0	0.20169	0.0	-0.20747	0.0	2.48	3.015673

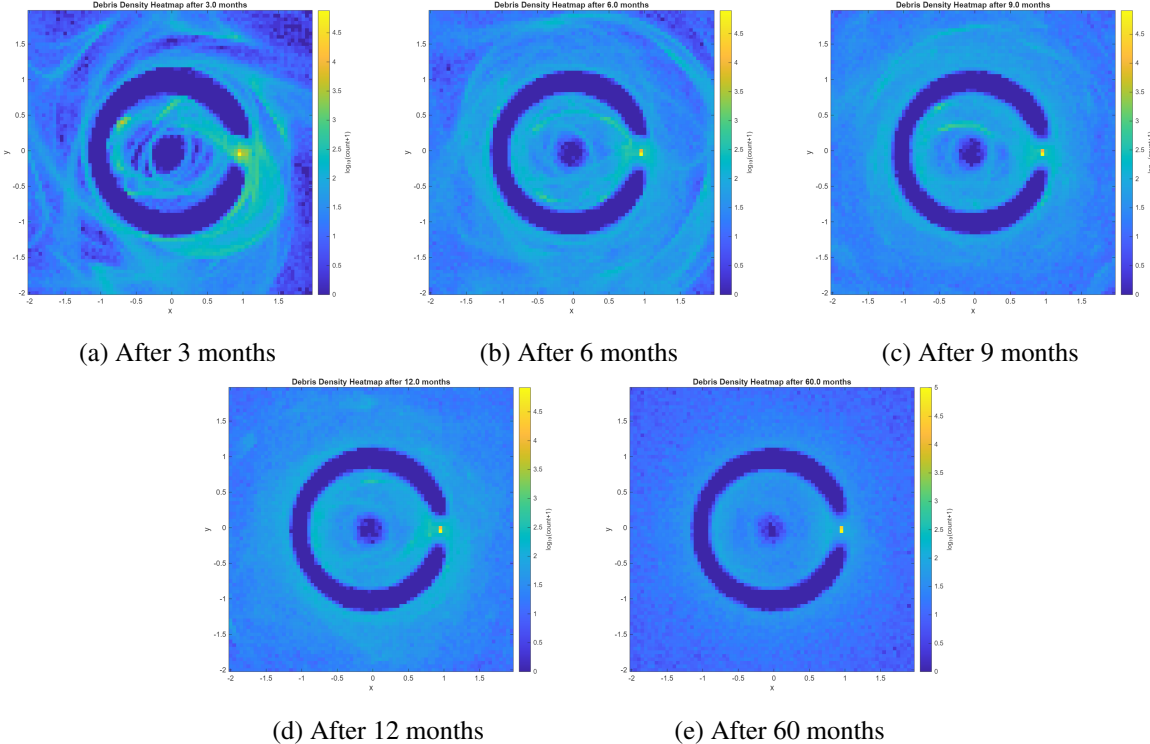


Figure 8: Debris Cloud Evolution over time following breakup at the NRHO

From the heatmaps in figure 8, we can also observe a general path taken by the fragments over time. It is also observed that the fragments bounce off the zero-velocity surfaces, which are very distinctly visible due to the spread of fragments.

4.2. Distant Retrograde Orbits

The DRO debris exhibits comparatively broader transport through the Earth–Moon system, consistent with its lower Jacobi constant (i.e., higher effective energy), which reduces the constraint imposed by the zero-velocity boundaries and enlarges the accessible regions of motion. Similar to the NRHO simulations, a total of 629,085 fragments of debris were simulated, and it was observed that only 7,612 of those fragments collided with the Lunar surface. Corresponding heatmaps are as seen in figure 9.

4.3. L₂ Halo Orbits

A total of 626,614 fragments of debris were simulated, and it was observed that 49,492 of those fragments collided with the Lunar surface. Corresponding heatmaps are as seen in figure 10. Similar to the NRHO simulations, we can observe a general path taken by the fragments over time, and the fragments also bounce off the zero-velocity surfaces, which are very distinctly visible due to the spread of fragments.

5. Discussion

5.1. Surveillance and Tracking

The Monte-Carlo breakup cases demonstrate that cis-lunar debris is not only a “local” hazard near the parent orbit; it is rapidly transported along dynamical structures of the Earth–Moon system. In all three scenarios,

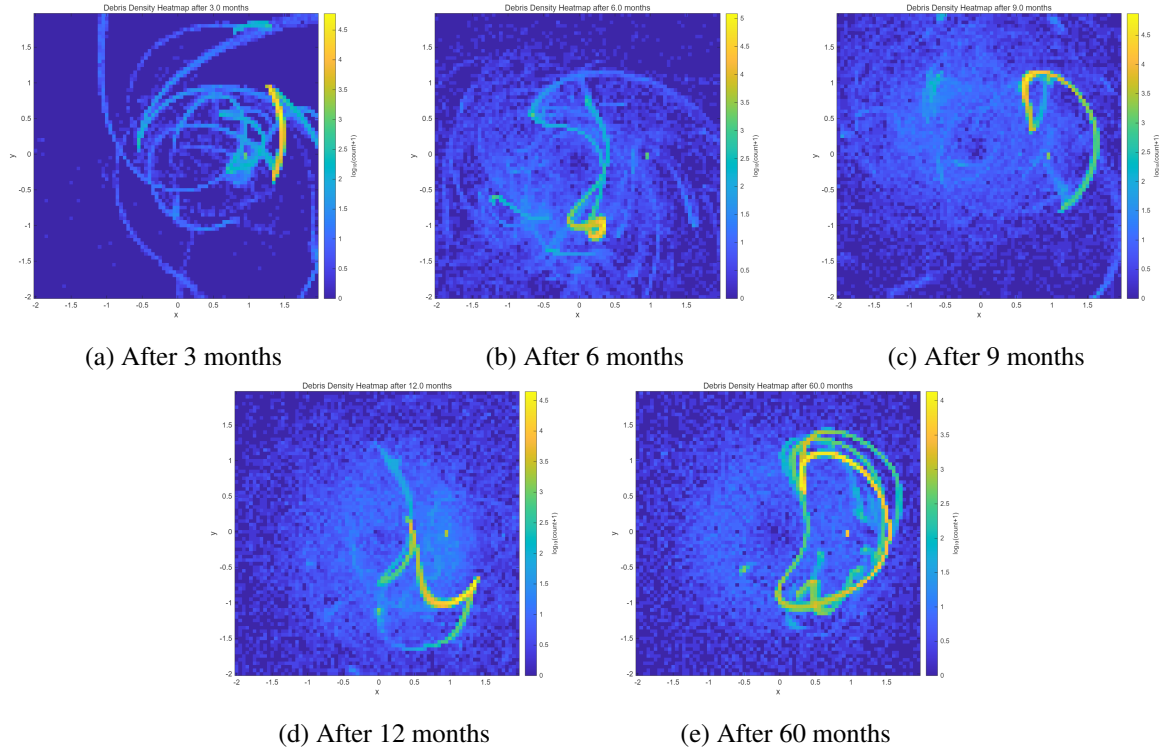


Figure 9: Debris Cloud Evolution over time following breakup at a DRO

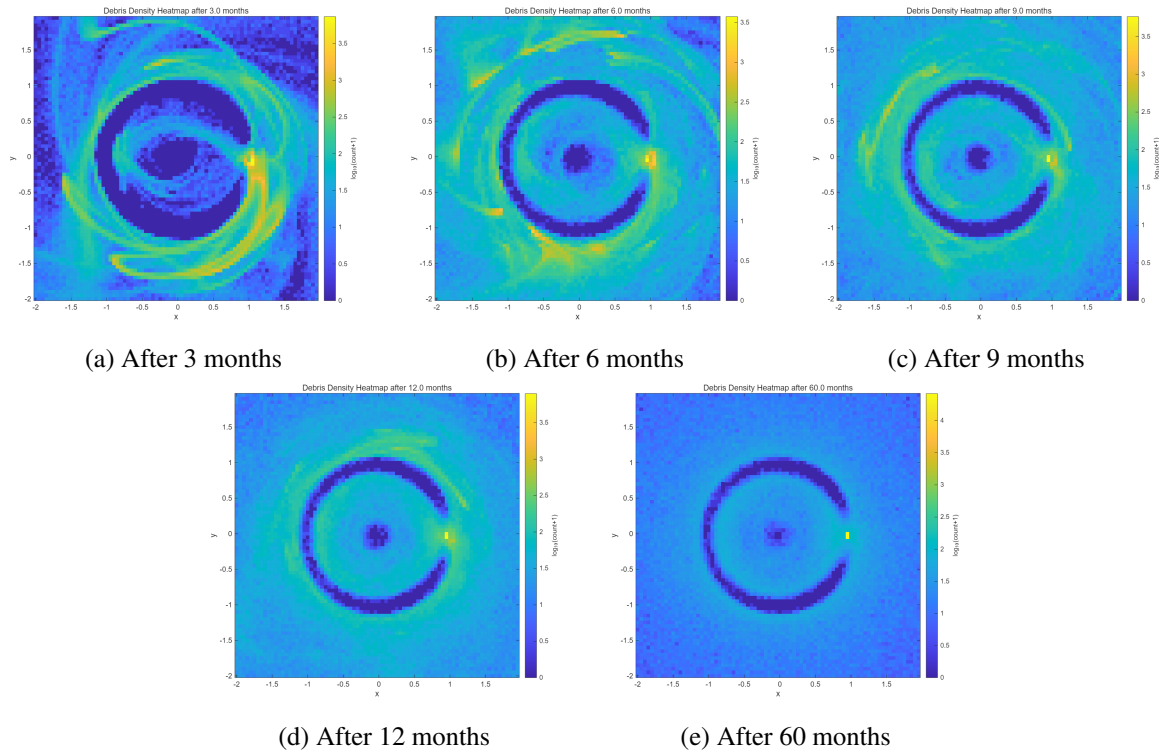


Figure 10: Debris Cloud Evolution over time following breakup at an L₂ Halo Orbit

Table 2: Number of Fragments Colliding with the Moon over time

Orbit Type	Number of Fragments	Lunar Impact	Percentage
NRHO	629,361	130,719	20.77%
DRO	629,085	7,612	1.21%
L ₂ Halo Orbit	626,614	49,492	7.90%

the cloud expands from an initially compact distribution (randomized within a 500 m radius) into coherent bands and voids that align with the accessible regions defined by the zero-velocity geometry and the orbit family of the parent trajectory. This is particularly evident in the NRHO and L₂ halo cases, where fragments appear to “bounce” and accumulate along zero-velocity boundaries, producing persistent high-density arcs rather than a uniformly mixed background.

From an SSA standpoint, this implies that a static sensor concept-of-operations (e.g., fixed pointing around the Gateway orbit) is insufficient. Instead, surveillance must be structured around (i) high-occupancy phase-space corridors that emerge in the heatmaps and (ii) time-evolving density peaks over the 3–60 month windows used here.

Practically, the simulations suggest two distinct tracking regimes:

- NRHO / L₂ halo vicinity tracking (asset protection mode): Both cases generate sustained concentrations near lunar distances, with substantial lunar impact counts indicating repeated close approaches to the Moon-facing region. In the NRHO case, 130,719 out of 629,361 simulated fragments strike the lunar surface over the simulation horizon, consistent with persistent lunar-proximal transport. In the L₂ halo case, 49,492 out of 626,614 fragments strike the lunar surface, again indicating strong coupling to the lunar neighborhood. This supports a surveillance posture that prioritizes conjunction screening for assets operating in/near these families and their transfer corridors.
- System-wide surveillance (environment characterization mode) for DRO-origin debris: DRO breakup produces relatively few lunar impacts (7,612 out of 629,085), but evolves toward a broad, near-spherical distribution across the Earth–Moon system at longer times, implying a diffuse but widespread background hazard with reduced predictability for “where the debris is concentrated” at any instant. This argues for wide-area survey strategies and periodic re-characterization of

the environment rather than only local keep-out screening.

Finally, the fragmentation and size assumptions used here frame a realistic “trackability gap” problem: fragments are sampled from 10 cm to 1 m, with large counts generated via EVOLVE-based scaling, and the model explicitly notes sensitivity to fragment size and reflectivity as relevant operational outputs. For many fragments in this regime, continuous catalog maintenance will likely require multi-sensor data fusion and predictive density mapping (heatmap-style products) rather than deterministic orbit maintenance for every object.

5.2. Mitigation Strategies

- Fragmentation prevention / passivation (highest leverage). Because the simulations show long-lived transport and system-wide spreading (especially in the DRO case), preventing breakup dominates downstream risk reduction. The study already assumes breakup types (collision/explosion) and uses EVOLVE-style fragment generation; operationally, this supports strict end-of-life passivation and fault-tolerant design to reduce explosion-like events.
- Keep-out zones and time-dependent conjunction screening. The abstract positions “keep-out zones and station-keeping choices” as near-term mitigations; your heatmaps provide the justification for making those zones dynamic (updated with time since breakup) rather than static geometric shells.
- Station-keeping policy tied to hazard fields. Since fragments concentrate along repeating arcs in NRHO/L₂-like motion, periodic station-keeping can be scheduled to avoid predicted high-density epochs (derived from the 3/6/9/12/60 month evolution you already compute).
- Design-for-survivability at critical nodes. Gateway-class assets in NRHO-relevant regions should treat the local debris environment as non-uniform and corridor-driven, aligning shielding orientation / operational attitudes with

the most probable approach directions inferred from the structured bands in the NRHO heatmaps.

6. Conclusions

This paper assessed the long-term evolution of cis-lunar debris clouds generated by breakup events in three representative Earth–Moon orbit families (NRHO, DRO, and an L₂ Halo), using EVOLVE-based Monte-Carlo fragment generation and multi-month to multi-year propagation with density heatmaps and lunar-impact flagging. Key findings include:

- Orbit family strongly governs debris fate and localization. For the NRHO case, 629,361 fragments were simulated and at least 130,719 impacted the lunar surface over the full propagation horizon, consistent with the orbit’s close lunar proximity. For the DRO case, 629,085 fragments were simulated and only 7,612 impacted the Moon. For the L₂ halo case, 626,614 fragments were simulated and 49,492 impacted the lunar surface.
- Transport is structured by CR3BP accessibility and zero-velocity boundaries. The debris clouds do not disperse uniformly; instead, their evolution exhibits corridor-like paths and sharp “walls” consistent with motion being constrained by the Jacobi constant and zero-velocity surfaces/curves. This manifests directly in the NRHO and L₂ halo simulations as fragments “bouncing” off the zero-velocity surfaces visible in the density plots.
- In the DRO case, the evolution trends toward a more global, near-spherical distribution across the Earth–Moon system, enabling less restricted motion.

This study used an EVOLVE-based size distribution with characteristic fragment lengths sampled between 10 cm and 1 m, with 1000 Monte-Carlo runs per orbit, and initial fragment positions randomized within 500 m of the parent. Fragments were propagated over 3, 6, 9, 12, and 60 months and assessed via heatmaps and lunar/Gateway-region flagging.

Future work should expand the current analysis in three complementary directions. First, the breakup campaign can be generalized beyond the single representative NRHO, DRO, and L₂ halo cases by sampling additional orbit families, energies, and phasing to quantify the sensitivity of debris transport, corridor occupancy, and lunar-impact likelihood to E and initial geometry. Second, incorporating higher-fidelity perturbations and

measurement modeling, such as ephemeris-based dynamics, solar radiation pressure, and realistic optical or radar detection constraints would enable the heatmap products presented here to be translated into trackability, catalog-maintenance, and conjunction-screening performance metrics. Third, the mitigation and end-of-life disposal concepts motivated by these results should be formulated as explicit targeting or optimal-control problems, with objectives such as minimizing ΔV and time-to-termination while avoiding repeated intersections with high-density transport corridors and the operational volumes associated with NRHO and L₂ trajectories.

Acknowledgements

The authors would like to thank Dr. Yosuke Kawabata from The University of Tokyo for his valuable insights and suggestions during the course of this work.

References

- [1] European Space Agency: *Recognising Sustainable Behaviour*, https://www.esa.int/Space_Safety/Space_Debris/Recognising_sustainable_behaviour, 2019.
- [2] Zubrin, R., *OP-ED | Lunar Gateway or Moon Direct?*, SpaceNews. <https://spacenews.com/op-ed-lunar-gateway-or-moon-direct/>, 2023.
- [3] Koon, W.S., Lo, M.W., Marsden, J.E., Ross, S.D. (2022) *Dynamical Systems, the Three-Body Problem and Space Mission Design*. Marsden Books, ISBN 978-0-615-24095-4.
- [4] Apetrii, M., Celletti, A., Efthymiopoulos, C., Galeş, C., Vartolomei, T. (2024). Simulating a breakup event and propagating the orbits of space debris. *Celestial Mechanics and Dynamical Astronomy*, 136(5), <https://doi.org/10.1007/s10569-024-10205-3>.